PERGAMON

International Journal of Heat and Mass Transfer 42 (1999) 1457–1466

International Journal of HEAT and MASS TRANSFER

Prediction of the critical heat flux in water subcooled flow boiling using a new mechanistic approach

G.P. Celata[a,*], M. Cumo[b], Y. Katto[c], A. Mariani[a]

[a] *ENEA, National Institute of Thermal-Fluid Dynamics, Via Anguillarese 301, 00060 S.M. Galeria, Rome, Italy*
[b] *University of Rome 'La Sapienza', Department of Nuclear Energy and Energy Conversion, C.so Vittorio Emanuele II, 198, 00100 Rome, Italy*
[c] *Nihon University, Department of Mechanical Engineering, Kanda-Surugadai 1–8, Chiyoda-ku, Tokyo 101, Japan*

Received 17 March 1998; in final form 17 July 1998

Abstract

A thorough examination of the results of existing models based on the liquid sublayer dryout theory suggested the need to postulate a new mechanism to predict the CHF in subcooled water flow boiling. Considering that we have local boiling with bulk subcooled conditions, there will be a distance from the wall at which the fluid temperature is equal to the saturation value. This distance is called 'superheated layer', and is the only region where a bubble may exist. Because of the accumulation and condensation of the vapour generated from the heated wall, a thin elongated bubble, called a 'vapour blanket', is formed, rising along the near-wall region as vertical distorted vapour cylinders. The CHF is postulated to occur when the vapour blanket replenishes the superheated layer, coming into contact with the heated wall (superheated layer vapour replenishment model).

The vapour blanket thickness, assumed to be equal to the bubble diameter at the wall detachment, is independent of the heat flux, depending on physical properties, thermal-hydraulic and geometric parameters. The superheated layer depends on the heat flux, physical properties, thermal-hydraulic and geometric parameters. The heat flux for which the superheated layer is equal to the vapour blanket thickness will be the CHF.

The comparison of new model predictions with fusion reactor relevant data ($0.1 \leqslant p \leqslant 8.4$ MPa, $0.3 \leqslant D \leqslant 25.4$ mm, $0.0025 \leqslant L \leqslant 0.61$ m, $1 \leqslant G \leqslant 90$ Mg m^{-2} s^{-1}, $25 \leqslant \Delta T_{sub,in} \leqslant 255$ K) is pretty good, as more than 85% of the 1968 data are predicted within $\pm 25\%$, with a standard deviation of $\pm 16.6\%$. Besides, because of its structure, based on the heat balance method, the model is applicable to both peripheral uniformly and non-uniformly heated channels.

Nomenclature

CHF critical heat flux [W m^{-2}]
C_p specific heat at constant pressure [J kg^{-1} K^{-1}]
D diameter [m]
f friction factor, dimensionless
$f(\beta)$ function of contact angle = 0.02–0.03, dimensionless
f_{tt} twisted-tape friction factor, given by eqn (14), dimensionless
G mass flux [kg m^{-2} s^{-1}]
k thermal conductivity [W m^{-1} K^{-1}]
L length [m]
p pressure [MPa]
Pr Prandtl number: $C_p\,\mu/k$, dimensionless
Q group defined in eqn (7)
q'' heat flux [W m^{-2}]
R radius [m]
Re Reynolds number: GD/μ, dimensionless
S heat transfer surface [m^2]
T temperature [°C]
U_τ friction velocity: $(\tau_w/\rho_L)^{0.5}$ [m s^{-1}]
x steam quality, dimensionless
y distance from the heated wall [m]

* Corresponding author. Fax: 00 39 06 3048 3026; e-mail: celata@casaccia-enea.it

0017–9310/98/$ - see front matter
PII: S0017–9310(98)00286–5

y^* superheated layer [m]
y^+ non-dimensional distance from the heated wall, defined in eqns (9)–(12).

Greek symbols
β contact angle, dimensionless
Γ mass flow rate [kg s^{-1}]
γ twist tape ratio, the number of tube diameters per 180° twist in the tape, dimensionless
ε surface roughness [m]
μ dynamic viscosity [kg s^{-1} m^{-1}]
ρ density [kg m^{-3}]
σ surface tension [N m^{-1}]
τ_w wall shear stress [MPa].

Subscripts
B pertains to the vapour blanket
cal calculated
ex exit conditions
exp experimental
in inlet
L pertains to the liquid phase
m mean
sub pertains to subcooled conditions
w pertains to the wall.

1. Introduction

Critical heat flux (CHF) in subcooled forced convective boiling has been widely studied in the past, mainly in connection with the thermal hydraulic design of light water reactors (LWRs). In this case, the order of magnitude of heat fluxes to be removed is around 1 MW m^{-2} [1–3]. Recent studies conducted under fusion-reactor relevant conditions, i.e. of low-to-intermediate pressure (up to 5 Mpa), high liquid velocity (up to 40 m s^{-1}), high liquid subcooling (up to 250 K), and small-to-intermediate channel diameter (1–15 mm), as reviewed by Celata [4], clearly showed that the CHF mechanisms under these extreme conditions may be largely different from those observed in the past for LWRs. Besides, under such conditions very high CHF values may be experienced, up to some tens of MW m^{-2}, such as those encountered in the thermal hydraulic design of high heat flux components for fusion reactors.

So far, various mechanisms of CHF have been proposed for subcooled flow boiling, but recently, based on a common basic mechanism such as the dryout of a liquid sublayer between the heated wall and a blanketing vapour film, three mechanistic models were presented by Lee and Mudawar [5], Katto [6–8], and Celata et al. [9]. Such a mechanism proved to be the most reasonable approach for the prediction of the CHF in subcooled flow boiling, [10]. In spite of the apparent similarity, a detailed analysis of the above mentioned mechanistic models revealed how they are quite different from each other in their basic nature [11]. Such a thorough examination of the results of previously proposed liquid sublayer dryout models suggested the need to postulate a new CHF mechanism of much simpler nature, to predict the CHF in water subcooled flow boiling. If we consider the temperature distribution in the main stream we may find a distance from the wall at which the fluid temperature will be equal to the saturation value. We call this distance as 'superheated layer', which is the only region where a bubble may exist, as the liquid bulk is subcooled. The CHF is postulated to occur when the vapour produced in the near-wall region replenishes the superheated layer, thus coming into contact with the heated wall (superheated layer vapour replenishment model).

2. The proposed CHF model

The reference flow configuration is schematically illustrated in Fig. 1. Because of the accumulation and condensation of the vapour generated at the heated wall, a thin elongated bubble called a 'vapour blanket' is formed, also as a consequence of the coalescence of small bubbles rising along the near-wall region as vertical distorted vapour cylinders. As already assumed by Lee and Mudawar [5], the circumferential growth of the vapour blanket is supposed to be strongly limited by adjacent blankets and by the steep velocity gradient. It is therefore

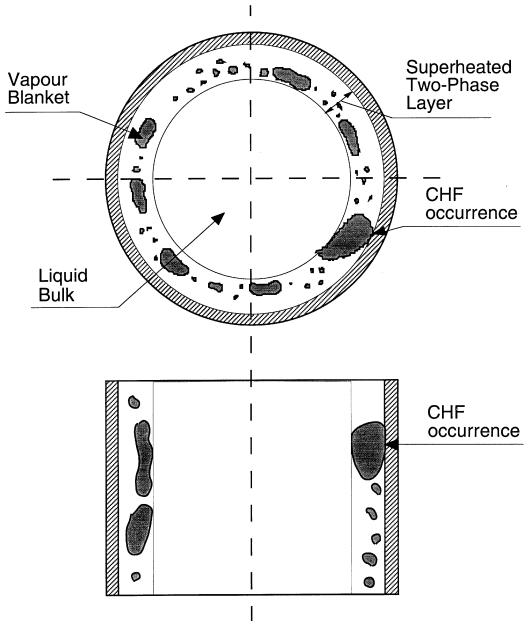

Fig. 1. Schematization of subcooled flow boiling near CHF conditions.

reasonable to assume the thickness of the vapour blanket, D_B, as approximately equal to the diameter of a bubble at the departure from the wall. The assumption is such that departing bubbles may coalesce into a distorted blanket that stretches along the fluid flow direction (due to vapour generation in the near-wall region) and keeps almost a constant thickness. A continuous blanket may be formed along the inner wall of the tube, as a consequence of blankets merging. The vapour blanket can develop and exist only in the near-wall region where the local liquid temperature is above the saturation value.

Considering the temperature distribution from the heated wall to the center of the channel, it will exist a distance from the wall, at which the temperature is equal to the saturation value at the local pressure. We define this distance as the 'superheated layer', and indicate it with y^*, as illustrated in Fig. 2. For a distance from the wall greater than y^*, the blanket (and each single bubble) will collapse in the subcooled liquid bulk. As initially suggested in [11], the CHF is postulated to occur when the vapour blanket replenishes the superheated layer, coming into contact with the heated wall, i.e. the heat flux for which y^* will be equal to D_B is assumed to be the CHF.

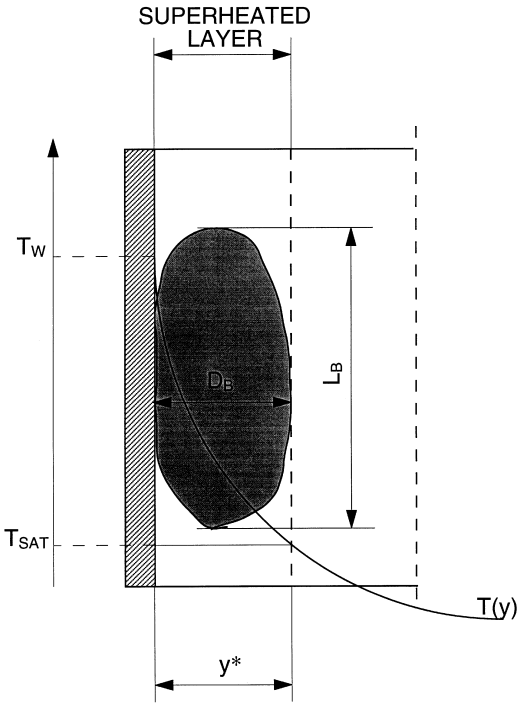

Fig. 2. Schematization of the superheated layer, i.e. the two-phase layer.

2.1. Calculation of the vapour blanket thickness

The evaluation of the vapour blanket thickness was made using the model proposed by Staub [12] to approximate the diameter of bubbles at departure. The Staub model is based on a balance of forces acting on growing bubbles attached to the heated surface. The bubble is considered to detach from the surface when dislodging forces overcome adhesive forces. Among the several forces acting on the bubble (surface tension force, dynamic force due to the momentum change of the liquid resulting from the growing bubble, drag force, buoyancy force, dynamic forces due to the liquid inertia and to the evaporating vapour thrust), Staub considered surface tension force (adhesive) and drag force (dislodging) to be the dominant. Then the balance of such forces yields the following expression for D_B:

$$D_B = \frac{32}{f}\frac{\sigma f(\beta)\rho_L}{G^2} \tag{1}$$

where β is the contact angle, and $f(\beta)$ is a function that depends only on contact angle. An approximate value for $f(\beta)$ of 0.02–0.03 for water was recommended, and $f(\beta) = 0.03$ is used in the present model. The friction factor f, is calculated using the Colebrook–White equation combined with Levy rough surface model [13], recommended for highly subcooled nucleate boiling. In fact, the pressure drop gradient will increase in the proximity of the CHF, as bubbles cause an increased surface roughness, but the coolant will still behave as a single-phase fluid. The expression for the friction factor is given by:

$$\frac{1}{\sqrt{f}} = 1.14 - 2.0\log\left(\frac{\varepsilon}{D} + \frac{9.35}{Re\sqrt{f}}\right) \tag{2}$$

where ε is the surface roughness, that has been shown to be close to 0.75 D_B, D is the inner tube diameter, and Re is the Reynolds number. Considering that $f(\beta) = 0.03$ and that $\varepsilon = 0.75D_B$, making use of eqn (1) the above equation may be rearranged as:

$$\frac{1}{\sqrt{f}} = 1.14 - 2.0\log\left(\frac{0.72\sigma\rho_L}{fDG^2} + \frac{9.35}{Re\sqrt{f}}\right) \tag{3}$$

Note the dependence of the friction factor on the surface tension. Solution of this equation for the friction factor requires iteration. Physical properties are calculated for saturation conditions at the exit pressure. Consequently, from eqn (1) D_B, and therefore the vapour blanket thickness, is independent of the heat flux, depending mainly on physical properties, thermal-hydraulic and geometric parameters.

2.2. Calculation of the superheated layer

The evaluation of the superheated layer in the near-wall region, i.e. the distance from the wall at which the temperature is equal to the saturation value, can be

obtained from the temperature distribution, as suggested by Martinelli [14]. The temperature T at a given distance from the wall, y, can be obtained for turbulent flow in a tube by:

$$T(y^+) = T_W - QPry^+ \quad 0 \leqslant y^+ < 5 \tag{4}$$

$$T(y^+) = T_W - 5Q\left\{Pr + \ln\left[1 + Pr\left(\frac{y^+}{5} - 1\right)\right]\right\} \quad 5 \leqslant y^+ < 30 \tag{5}$$

$$T(y^+) = T_W - 5Q\left[Pr + \ln(1+5Pr) + 0.5\ln\left(\frac{y^+}{30}\right)\right] \quad y^+ \geqslant 30 \tag{6}$$

with

$$U_\tau = \left(\frac{\tau_W}{\rho_L}\right)^{0.5} \quad y^+ = y\frac{U_\tau}{\mu_L}\rho_L \quad \tau_W = \frac{fG^2}{8\rho_L}$$

where T_W is the wall temperature, Pr is the liquid Prandtl number, y^+ is defined above, and Q is a group defined as a function of the local heat flux, q'', the liquid specific heat, C_{pL} and the friction velocity, U_τ:

$$Q = \frac{q''}{\rho_L C_{pL} U_\tau} \tag{7}$$

In the above eqn (7) C_{pL} is calculated at saturation conditions at the exit pressure. As the wall temperature T_W is not known (it can alternatively be calculated using empirical correlations), we may proceed as follows. We may calculate the exit average temperature of the fluid, T_m with two independent equations. The first one is the heat balance in the fluid, which for a given heat flux q'' yields:

$$T_m = T_{in} + \frac{q''S}{\Gamma C_{pL}} \tag{8}$$

where T_{in} is the liquid inlet temperature, S is the heat transfer surface ($S = \pi DL$), and Γ is the mass flow rate. In eqn (8), C_{pL} is calculated at the average temperature along the channel. The second independent equation to calculate T_m is given by the integration along the radius of eqns (4)–(6):

$$T_m = \frac{5}{y^+(R)}T_{m1} + \frac{25}{y^+(R)}T_{m2} + \frac{y^+(R)-30}{y^+(R)}T_{m3} \tag{9}$$

with

$$T_{m1} = \frac{1}{5}\int_0^5 T(y^+)\,dy^+ \quad 0 \leqslant y^+ < 5 \tag{10}$$

$$T_{m2} = \frac{1}{25}\int_5^{30} T(y^+)\,dy^+ \quad 5 \leqslant y^+ < 30 \tag{11}$$

$$T_{m3} = \frac{1}{y^+(R)-30}\int_{30}^{y^+(R)} T(y^+)\,dy^+ \quad y^+ \geqslant 30 \tag{12}$$

R being the radius of the channel. In eqns (8) and (9), T_W is the only unknown and, therefore, it can be easily determined. Once T_W is known, it will be possible to calculate the distance from the wall y, at which the liquid temperature is equal to the saturation value at the local pressure, i.e. the superheated layer y^*. This procedure allows to obtain the wall temperature, and consequently the superheated layer y^*, directly from the heat balance. No use of empirical correlations is made for the evaluation of the heat transfer coefficient, and also new empirical constants are avoided. It accounts for inlet subcooling and, through eqn (8), makes the model immediate to be used for peripheral non-uniform heating. This can be done by properly considering as $q''S$ the total power delivered to the fluid, independent of its peripheral distribution. The superheated layer y^* depends on the heat flux, physical properties, thermal-hydraulic and geometrical parameters.

2.3. Critical heat flux

The CHF, for given geometric and inlet thermal-hydraulic conditions, and local pressure p (at the CHF section), is the heat flux for which the following equation is verified:

$$y^* = D_B \tag{13}$$

Solution of eqn (13) can be obtained by an iterative calculation through the foregoing eqns (1)–(12). Physical properties are calculated at saturation conditions, unless otherwise specified. Figure 3 shows the trends of D_B and y^* as a function of the heat flux during the calculation. As already stated above, D_B is independent of the heat flux, while y^* is an increasing function of it.

3. Verification of the CHF model

To verify the accuracy of the proposed model, a CHF data set of 1968 data points gathered by authors for

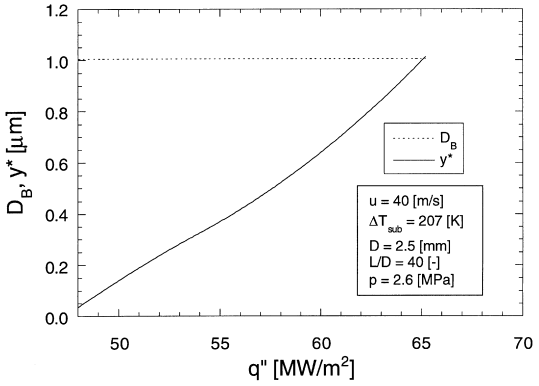

Fig. 3. Trend of the vapour blanket thickness D_B and superheated layer y^* vs the heat flux during the calculation.

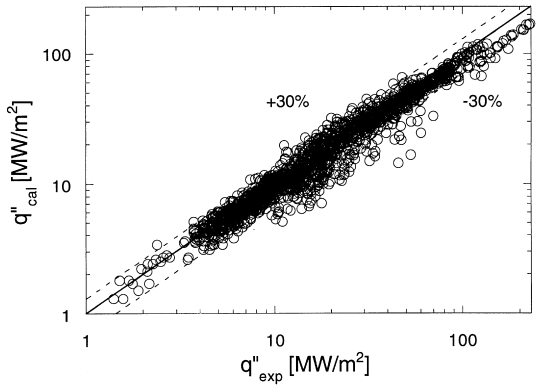

Fig. 4. Calculated vs experimental CHF using the whole data set [15].

operating ranges typical of fusion reactor thermal-hydraulics has been used [15]. It is characterized by the following operating ranges: $0.1 \leqslant p \leqslant 8.4$ MPa; $0.3 \leqslant D \leqslant 25.4$ mm; $0.0025 \leqslant L \leqslant 0.61$ m; $1 \leqslant G \leqslant 90$ Mg m^{-2} s^{-1}; $25 \leqslant \Delta T_{\text{sub,in}} \leqslant 255$ K. Such a data base refers to peripheral and axial uniform heating in smooth channels.

Figure 4 shows a comparison of calculated vs experimental CHF, using the above data set. About 85% of data points are predicted within $\pm 25\%$, while more than 90% of the 1968 data points used are predicted within $\pm 30\%$. The standard deviation is $\pm 16.6\%$. This is a very good performance, also taking into account the wide operating ranges of the data set.

It is of interest making a comparison between the prediction of the same data set obtained using the superheated layer vapour replenishment model (the present one), and the liquid sublayer dryout theory according to the Celata et al. model [9]. Such a comparison is shown in Fig. 5, where the ratio between the calculated and the experimental CHF is plotted vs the exit quality for the two models. The global trend is quite the same for the two models, being very difficult to distinguish their prediction for same data points. Also statistics are very similar, where the Celata et al. model [9] predicts about 91% of data points within $\pm 30\%$, with a standard deviation of 16.4%.

Although the basic mechanisms, which the two foregoing models rely on, are significantly different, they use exactly the same equations to calculate the vapour blanket thickness and the superheated layer. Of course, the closure equation, connected with the different mechanism leading to CHF, is different in the two models. The superheated layer vapour replenishment model is definitely simpler than the liquid sublayer dryout model in its mathematical formulation and calculation procedure, none-the-less providing exactly the same performance in the prediction of the same data set. Likely to the liquid sublayer dryout model, the present model shows a systematic underprediction of the CHF for those data characterized by exit conditions close to the saturation. It is obvious that approaching the saturation conditions, assumptions made in the construction of the model may not hold any longer, and the model provides a systematic error in the prediction. Figure 6, where the calculated-to-experimental CHF ratio is plotted vs inlet subcooling, shows, of course, a similar though inverse trend than that reported in Fig. 5, providing the limits of the model in terms of inlet subcooling, which is an input parameter.

Further plots shown in Figs 7–10 demonstrate the absence of any other significant systematic effect in the present model predictions. In these figures, the ratio between the calculated and the experimental CHF is plotted vs mass flux, G, pressure, p, channel diameter, D, and channel L/D, respectively. From Figs 7–10, the only concern may be in the very slight underprediction of the CHF for G lower than 2000 kg m^{-2} s^{-1} and for D lower than 0.5 mm. Such conditions refer to situations where the CHF is not so high and is generally associated with

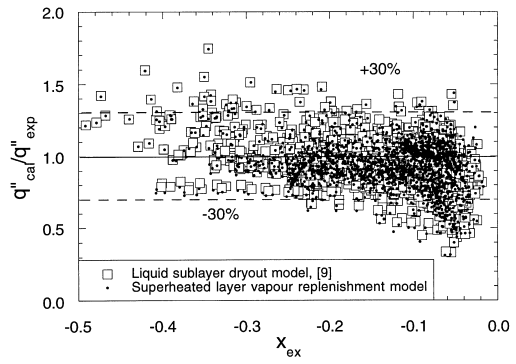

Fig. 5. Ratio of the calculated to the experimental CHF vs exit quality for the present model and the Celata et al. model [9].

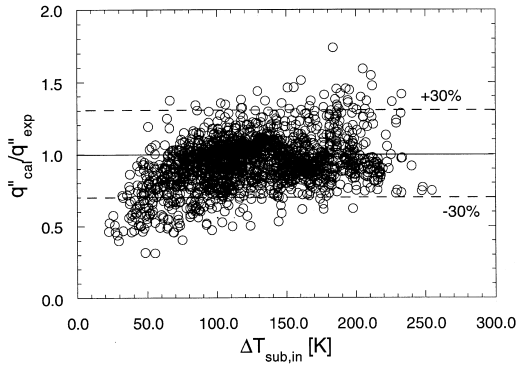

Fig. 6. Ratio of the calculated to the experimental CHF vs inlet subcooling.

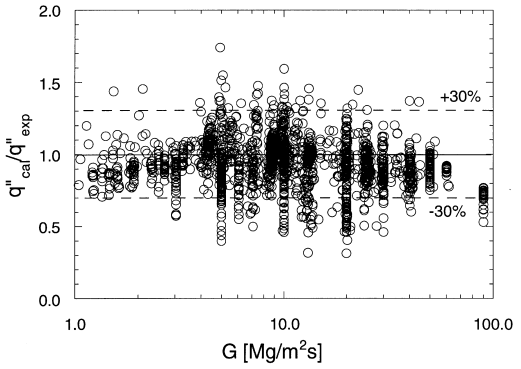

Fig. 7. Ratio of the calculated to the experimental CHF vs mass flux.

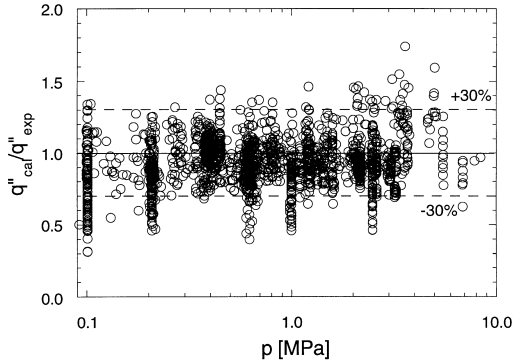

Fig. 8. Ratio of the calculated to the experimental CHF vs exit pressure.

slightly subcooled conditions ($G < 2000$ kg m^{-2} s^{-1}), or to extreme geometric constraints for which different CHF mechanisms may be hypothesized ($D < 0.5$ mm [16]). None-the-less, no systematic effect is generally found for max flux, pressure, channel diameter and length.

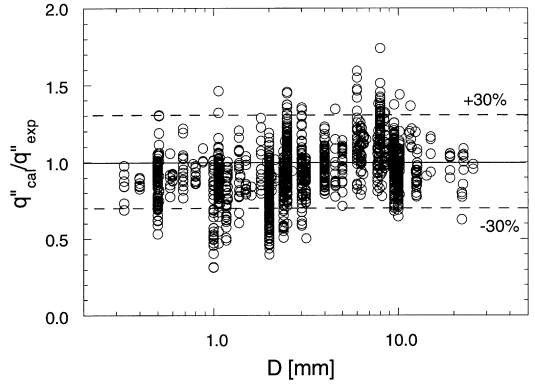

Fig. 9. Ratio of the calculated to the experimental CHF vs channel diameter.

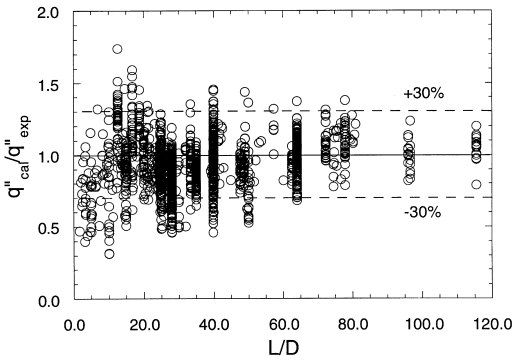

Fig. 10. Ratio of the calculated to the experimental CHF vs length-to-diameter ratio.

Just to have an idea of the calculated values of the superheated layer, y^*, and vapour blanket thickness, D_B, in Fig. 11 we plotted the calculated-to-experimental CHF ratio vs D_B or y^* at the CHF. Larger errors (greater than $\pm 30\%$) are concentrated in the region of very small values of D_B and y^*, where uncertainty is obviously greater.

4. Parametric trends

It is of interest to verify the parametric trends of the model for the subcooled CHF. This latter is a function of thermal hydraulic conditions (mass flux, pressure and subcooling) and geometric parameters (channel diameter and length). The parametric trends of subcooled CHF at medium/low pressure, very high mass flux, high and very high subcooling, and small/very small tube diameter, typical of fusion reactor thermal hydraulics, can be summarized as follows:

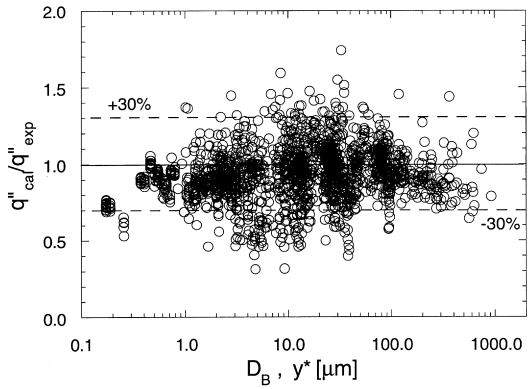

Fig. 11. Ratio of the calculated to the experimental CHF vs the calculated values of the vapour blanket thickness D_B and superheated layer y^*.

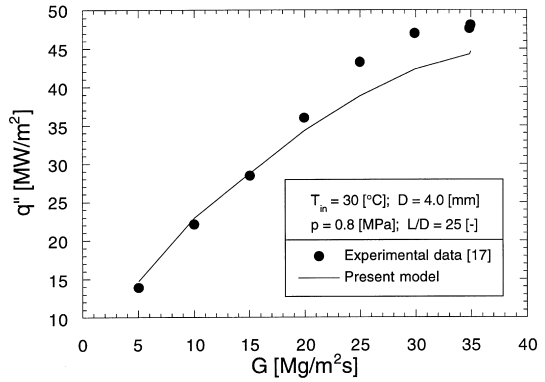

Fig. 12. Mass velocity effect on CHF.

- CHF increases as mass flux increases.
- CHF is practically independent of the pressure.
- CHF increases with increasing degree of subcooling.
- CHF increases as tube diameter decreases.

Figures 12–15 show the calculated and the experimental CHF vs mass flux, pressure, inlet subcooling and exit quality, and tube diameter, respectively, for typical data points selected from the high heat flux data set. Figure 12 shows that the model provides the same observed experimental trend of CHF vs mass flux, for a wide range of G [17]. The negligible dependence of CHF on exit pressure is matched by the model at low pressure [18] and medium pressure [40], as shown in Fig. 13. The almost linear dependence of the CHF on the liquid subcooling is verified in Fig. 14, where the CHF is plotted vs inlet subcooling [19, 20] (top figure) and exit quality [19–23] (bottom figure). The dependence of the CHF on D at small diameters is well predicted by the model, as shown in Fig. 15, together with the inter-relation between tube inside diameter and liquid velocity.

The parametric trends shown in Figs 12–15, demonstrate that the proposed model is very accurate in predicting independent CHF variations with respect to mass flux, pressure, liquid subcooling and channel diameter in the range of high heat fluxes, i.e. high mass flux and high subcooling.

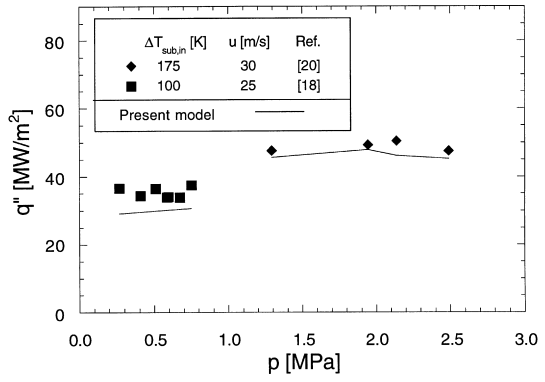

Fig. 13. Pressure effect on CHF.

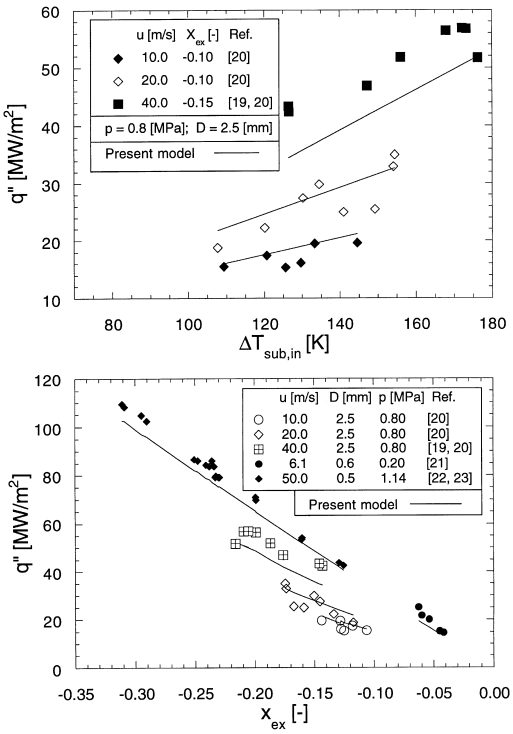

Fig. 14. Inlet subcooling (top figure) and exit quality effect (bottom figure) on CHF.

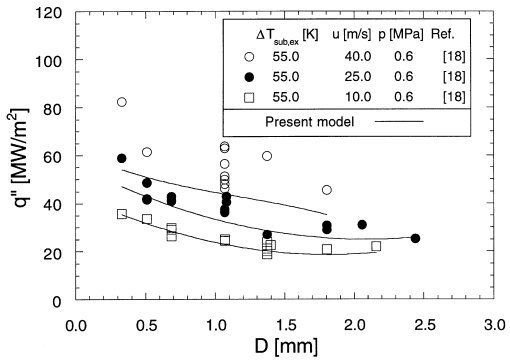

Fig. 15. Diameter effect on CHF.

5. Peripheral non-uniform heating and swirl flow

Like the Celata et al. model [9], based on the liquid sublayer dryout theory, the present model can be also

used to predict the CHF under peripheral non-uniform heating conditions of the channel. The effect of non-uniform heating along the circumference of the tube can be of relevant importance in the thermal hydraulic design of fusion reactors high heat flux components. In fact, as an example, the divertor is thermally loaded only on one side. Circumferential non-uniform heating can be accounted for in the model description simply by considering the total thermal power delivered to the fluid in the coolant heat balance for the calculation of the local average coolant temperature, eqn (8). It is evident that average bulk thermal hydraulic conditions, which the CHF is strongly dependent on, are only a function of the total thermal power delivered to the fluid, independent of its distribution. As boiling crisis in subcooled flow boiling depends on local thermal-hydraulics conditions [4], all equations employed in the model mathematical description can be used also in the case of peripheral non-uniform heating. In fact, all calculations, except for the cross-section average temperature, are made using the maximum value of the heat flux, and all parameters used to calculate the CHF are local values. Temperature and velocity distributions are still valid in the sector interested by the heat flux. A possible distortion of such distributions is likely to happen in the bulk of the flow, due to turbulent mixing. As velocity and temperature distributions are used locally in the calculation of the CHF, it looks reasonable to continue in making use of such distributions, also in the case of peripheral non-uniform heating. The prediction of the Gaspari data [24] is shown in Fig. 16, where the ratio between the calculated and the experimental critical heat flux is plotted vs the exit quality, x_{ex}. The agreement is good, being most of the 26 experimental data within $\pm 20\%$.

Although very high heat fluxes, such as those requested for fusion reactors applications, could be physically obtained using water subcooled flow boiling in straight tubes, none-the-less engineering considerations limit the variation of parameters such as velocity, channel diameter and liquid subcooling. On the other hand, safety margins call for suitable techniques to further enhance the upper limit of the heat transfer, i.e. the CHF. Recent experiments showed that use of twisted tapes as swirl flow promoters in water subcooled flow boiling proved to be very effective in the CHF enhancement, allowing an increase in the CHF up to a factor of 2.0 [25, 26].

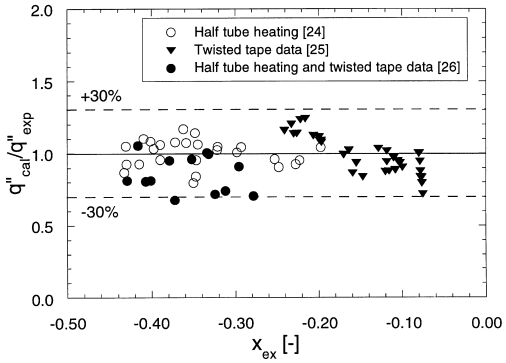

Fig. 16. Prediction of peripheral non-uniform heating, straight flow CHF data [24]; uniform heating, swirl flow CHF data [25]; swirl flow, peripheral non-uniform heating CHF data [26], vs exit quality.

The present model may be used to predict CHF swirl flow data, making use of the same corrections already used in empirical correlations. As the presence of a twisted tape inside a channel is associated with a relevant increase in the pressure drop (e.g. up to a factor of 11 in [26]), a friction factor correction for twisted tapes was suggested by Lopina and Bergles [27]. Based on experiments, Lopina and Bergles show that the friction factor, f_{tt}, for use in the twisted tape geometry varies as:

$$f_{tt} = 2.75 f \gamma^{-0.406} \tag{14}$$

where γ is the twist ratio of the tape, a measure of the number of tube diameters per 180° twist in the tape, and f is the friction factor for straight tube. To extend the present model for use with twisted tapes, eqn (14) was tried.

The prediction of Nariai et al. data [25] is shown in Fig. 16. The agreement is quite encouraging as almost all the data are predicted within $\pm 25\%$, showing that the procedure can be successful.

Recent experiments by Cardella et al. [26] were carried out with twisted tapes inserted in peripherally half-heated tubes. Predictions obtained with the present model on these data are shown again in Fig. 16. The agreement can be considered satisfactory in view of the complexity of the situation in comparison with the original description of the model. Although a general slight underestimation of the CHF is observed, most of the experimental data are predicted within $\pm 25\%$.

6. Low mass flux–high pressure data

Although the model is developed for high mass flux, high liquid subcooling and low/medium pressure conditions, it is of interest to verify its validity under different operating conditions, provided exit subcooled conditions still exist. As already said, subcooled flow boiling CHF was experimentally investigated in the past with reference to pressurized water reactors, i.e. low mass flux, high pressure and low liquid subcooling (collections of data are reported in [28–30]).

Assumptions which the model is based on, rely on the hypothesis that the mass flux is sufficiently high (greater than 2–3000 kg m^{-2} s^{-1}) and exit thermal hydraulic conditions are not so close to the saturation ones (let us say $x_{ex} < -0.1$). It is evident that a mass flux lower than the

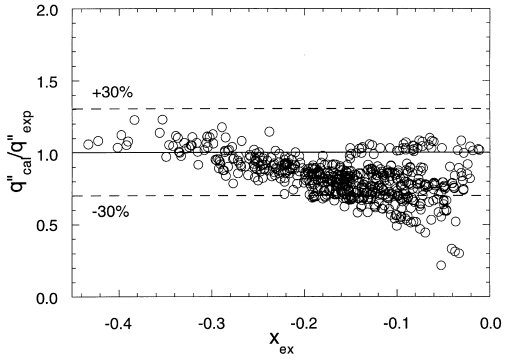

Fig. 17. Prediction of low mass flux–high pressure CHF data [28–30] vs exit quality.

above limits may worsen the performances of the model, reducing its capability to predict the CHF in subcooled flow boiling to $x_{ex} < -0.2$ or less. The prediction of the experimental data gathered in [28–30] using the present model is shown in Fig. 17, where, as usual, the calculated-to-experimental CHF ratio is plotted vs exit quality, x_{ex}. The overall operating ranges of such data are as follows: $350 < G < 18600$ kg m^{-2} s^{-1}, $1.38 < p < 20.7$ MPa, $1.14 < D < 37.5$ mm, $11.7 < L/D < 365.3$, $-0.664 < x_{ex} < -0.044$, $1.1 <$ CHF < 21.4 MW m^{-2}.

The performance of the present model with the above data is as expected. A reasonable agreement with experimental data is shown as far as exit thermodynamic conditions are not so close to the saturated state. The threshold in terms of x_{ex} depends on mass flux and ranges from $x_{ex} = -0.2$ (very low mass flux) to $x_{ex} = -0.1$ (low mass flux).

However, globally, for a total of 654 data points, the rms is 22.4%, while 71.0% of data lie within $\pm 25\%$ (83.3% of data lie within $\pm 30\%$).

7. Conclusions

A new mechanistic model has been developed for the prediction of the CHF in water subcooled flow boiling. It is specifically thought to predict the CHF under conditions of high mass flux, intermediate-to-low pressure (below 8.4 MPa), and high liquid subcooling, typical of the thermal hydraulic design of fusion reactor high heat flux components. None-the-less, it is able to predict the CHF over a wide range of subcooled conditions.

The model is based on the observation that, during vigorous subcooled boiling, a vapour blanket forms in the vicinity of the heated wall because of the coalescence of small bubbles. Depending on the heat flux, a more or less steep temperature gradient exists in each section. Because of bulk subcooled conditions, there will be a distance from the heated wall at which the fluid temperature is equal to the saturation value, and we call this distance superheated layer. The CHF is assumed to occur when the superheated layer is replenished by vapour, which comes into contact with the heated wall and causes the burnout.

The model has been tested over a large subcooled flow boiling CHF data bank (almost 2000 data points) characterized by wide ranges of operating conditions, showing a generally good accuracy in the prediction of experimental data. The model looses its validity when local thermodynamic conditions at the CHF approach the saturated state of the liquid bulk.

Although the model is developed for peripheral uniform heating, it can easily account for circumferential non-uniform heat distribution. This is done considering the total thermal power delivered to the fluid in the coolant heat balance for the calculation of the local average thermal hydraulic conditions. In addition, using a simple correction for the friction factor, the model provides also a good prediction of swirl flow data obtained with twisted-tape inserts, showing a good capability in predicting also the complex situation given by the simultaneous occurrence of swirl flow and peripheral non-uniform heating.

References

[1] A.E. Bergles, J.G. Collier, J.M. Delhaye, G.F. Hewitt, F. Mayinger, Two-Phase Flow and Heat Transfer in the Power and Process Industries, Hemisphere Publishing Corporation, New York, 1981, pp. 226–255.
[2] J.G. Collier, Convective Boiling and Condensation, 2nd ed., McGraw–Hill, New York, 1981, pp. 144–177.
[3] Y.Y. Hsu, R.W. Graham, Transport Processes in Boiling and Two-Phase Systems, American Nuclear Society, 1986, pp. 217–232.
[4] G.P. Celata, Critical heat flux in water subcooled flow boiling; experimentation and modelling, Proceedings of the Second European Thermal-Sciences and 14th UIT National Heat Transfer Conference, vol. 1, 1996, pp. 27–40.
[5] C.H. Lee, I.A. Mudawar, A mechanistic critical heat flux model for subcooled flow boiling based on local bulk flow conditions, Int. J. Multiphase Flow 14 (1998) 711–728.
[6] Y. Katto, A physical approach to critical heat flux of subcooled flow boiling in round tubes, Int. J. Heat Mass Transfer 33 (1990) 611–620.
[7] Y. Katto, Prediction of critical heat flux of subcooled flow boiling in round tubes, Int. J. Heat Mass Transfer 33 (1990) 1921–1928.
[8] Y. Katto, A prediction model of subcooled water flow boiling chf for pressure in the range 0.1–20 MPa, Int. J. Heat Mass Transfer 35 (1992) 1115–1123.
[9] G.P. Celata, M. Cumo, A. Mariani, M. Simoncini, G. Zummo, Rationalization of existing mechanistic models for the prediction of water subcooled flow boiling critical heat

flux, Int. J. Heat Mass Transfer 37 (Suppl. 1) (1994) 347–360.
[10] G.P. Celata, Modelling of critical heat flux in subcooled flow boiling, Proceedings of the Convective Flow and Pool Boiling Conference, Irsee, 1997.
[11] Y. Katto, Synthetic view of the chf mechanism in subcooled flow boiling based on the recent mechanistic models, Proceedings of the Convective Flow and Pool Boiling Conference, Irsee, 1997.
[12] F.W. Staub, The void fraction in subcooled boiling—prediction of vapour volumetric fraction, J. Heat Transfer 90 (1968) 151–157.
[13] S. Levy, Forced-convection subcooled boiling prediction of vapour volumetric fraction, Int. J. Heat Mass Transfer 10 (1967) 951–965.
[14] R.C. Martinelli, Heat transfer to molten metals, Trans. ASME 69 (1947) 947–951.
[15] G.P. Celata, A. Mariani, A data set of critical heat flux in water subcooled flow boiling, in: J. Schlosser (Ed.), Proceedings of the Third International Workshop on High Heat Flux Components Thermal Hydraulics in Fusion Reactors, 1993.
[16] G.P. Celata, M. Cumo, A. Mariani, Geometrical effects on the subcooled flow boiling critical heat flux, Proceedings of the Fourth World Conference on Experimental Heat Transfer, Fluid Mechanics, and Thermodynamics, vol. 2, 1997, 867–872.
[17] G.P. Celata, M. Cumo, A. Mariani, Technical Report, ENEA (classified).
[18] C.L. Vandervoort, A.E. Bergles, M.K. Jensen, The ultimate limits of forced convective subcooled boiling heat transfer, Technical Report, HTL-9, RPI, 1990.
[19] G.P. Celata, M. Cumo, A. Mariani, Experimental results on high heat flux burnout in subcooled flow boiling, Energia Nucleare 10 (1) (1993) 46–57.
[20] G.P. Celata, M. Cumo, A. Mariani, Burnout in highly subcooled flow boiling in small diameter tubes, Int. J. Heat Mass Transfer 36 (1991) 1269–1285.
[21] C.S. Loosmore, B.C. Skinner, Subcooled critical heat flux for water in round tube, S.M. thesis, Massachusetts Institute of Technology, Cambridge, Massachusetts, 1965.
[22] A.P. Ornatskii, L.S. Vinyarskii, Heat transfer crisis in a forced flow of underheated water in small bore tubes, Teplofizika Vysokikh Temperatur (High Temperature) 3 (1964) 444–451.
[23] A.P. Ornatskii, The influence of length and tube diameter on critical heat flux for water with forced convection and subcooling, Teploenergetika 4 (1960) 67–69.
[24] G.P. Gaspari, Comparison among data of electrically and e-beam heated tubes, in: J. Schlosser (Ed.), Proceedings of the Third International Workshop on High Heat Flux Components Thermal Hydraulics in Fusion Reactors, 1993.
[25] H. Nariai, F. Inasaka, W. Fujisaki, H. Ishiguro, Critical heat flux of subcooled flow boiling in tubes with internal twisted tapes, Proceedings of the ANS Winter Meeting (THD), 1991, pp. 38–46.
[26] A. Cardella, G.P. Celata, G. Dell'Orco, G. Gaspari, G. Cattadori, A. Mariani, Thermal hydraulics experiments for the NET divertor, Proceedings of the 17th Symposium on Fusion Technology, vol. 1, 1992, pp. 206–210.
[27] R.F. Lopina, A.E. Bergles, Heat transfer and pressure drop in tape-generated swirl flow of single-phase water, J. Heat Transfer 91 (1969) 8–13.
[28] C.L. Williams, S.G. Beus, Critical heat flux experiments in a circular tube with heavy water and light water, Technical Report, WAPD-TM-1462, Westinghouse, 1980.
[29] J.M. Robertson, Heat transfer to high pressure steam water mixtures, Technical Report, HTFS-DR 6, HTFS Company, 1971.
[30] B. Thompson, R.V. Macbeth, Boiling water heat transfer—burnout in uniformly heated round tubes: a compilation of world data with accurate correlations, AEEW-R 356, 1964.